

An Eigenvalue Ratio Approach to Inferring Population Structure from Large-scale Sequencing Data

Yuyang Xu, Jianfeng Yao, and Zhonghua Liu*

Department of Statistics and Actuarial Science, University of Hong Kong

August 13, 2021

Abstract

Inference of population structure from genetic data plays an important role in population and medical genetics studies. The traditional EIGENSTRAT method has been widely used for computing and selecting top principal components that capture population structure information (Price et al., 2006). With the advancement and decreasing cost of sequencing technology, whole-genome sequencing data provide much richer information about the underlying population structures. However, the EIGENSTRAT method was originally developed for analyzing array-based genotype data and thus may not perform well on sequencing data for two reasons. First, the number of genetic variants p is much larger than the sample size n in sequencing data such that the sample-to-marker ratio n/p is nearly zero, violating the assumption of the Tracy–Widom test used in the EIGENSTRAT method. Second, the EIGENSTRAT method might not be able to handle the linkage disequilibrium (LD) well in sequencing data. To resolve those two critical issues, we propose a new statistical method called ERStruct to estimate the number of latent sub-populations based on sequencing data. We propose to use the ratio of successive eigenvalues as a more robust testing statistic, and then we approximate the null distribution of our proposed test statistic using modern random matrix theory. Simulation studies found that our proposed ERStruct method has outperformed the traditional Tracy–Widom test on sequencing data. We further use two public data sets from the HapMap 3 and the 1000 Genomes Projects to demonstrate the performance of our ERStruct method. We also implement our ERStruct in a MATLAB toolbox which is now publicly available on GitHub: <https://github.com/bglvly/ERStruct>.

Keywords: Eigenvalue ratio; Linkage disequilibrium; Population structure; Random matrix; Sequencing data.

*To whom correspondence should be addressed: zhhlui@hku.hk

1 Introduction

Inference of population structure is a fundamentally important problem in population genetics and also plays a critical role in genetic association studies (Novembre et al., 2008; Skoglund et al., 2017; Cao et al., 2020). Principal component analysis (PCA) based method has been popularized to capture the population structures from array-based genotype data (Menozzi et al., 1978; Patterson et al., 2006; Reich et al., 2008). PCA works by selecting top principal components (PCs) that can sufficiently capture population structures, and then those top PCs can be further used to correct for population stratification bias in genetic association studies, for example, using the popular EIGENSTRAT method (Price et al., 2006).

A natural and necessary question when applying PCA on genetic data is to determine the number of PCs that can sufficiently capture the underlying unknown population structure. Patterson et al. (2006) developed the so-called sequential Tracy–Widom test using the “effective number of markers” as a plug-in estimate of the original number of markers in the data set. The effective number of markers is then used to estimate the number of the underlying uncorrelated markers so that the number of markers can be effectively reduced. With the use of effective number of markers, Patterson et al. (2006) tried to alleviate the possible violation of the assumption in the Tracy–Widom test that the sample size and the number of genetic markers should be comparably large. We will refer to this method as the PCA-TW test throughout this paper.

However, after being applied in various empirical studies for several years, it has been found that the PCA-TW test might not perform well for capturing the true population structure in sequencing data (Song et al., 2015; Prokopenko et al., 2015; Zhang et al., 2020). This is because the traditional PCA-TW test was originally developed for array-based genotype data sets that typically contain a moderate-to-high number of genetic markers, while the number of genetic markers is much larger in sequencing data. As large-scale sequencing data sets become increasingly available, we need to develop a new method that can resolve the following two important and unsolved issues:

1. *Linkage disequilibrium* (LD). Markers within a genotype sequencing data set may

have very high correlations (0.6–0.9). This issue becomes even worse when markers are close to each other. The theoretical validity of the PCA-TW test requires the independence assumption among the genetic markers. Hence, the presence of LD may seriously distort the null distribution of the test statistic and thus leads to biased inference. [Patterson et al. \(2006\)](#) recommended a modification of their PCA-TW test method using backward regression to correct for the presence of LD. However, this correction is computationally intensive, especially when a wide range of genetic markers are in LD with each other. Another method is LD pruning or clumping ([Purcell et al., 2007](#); [Palla and Dudbridge, 2015](#)) which only selects genetic variants that are uncorrelated in an LD block by removing all the other genetic variants. This data filtering method apparently will result in a substantial loss of information about population structures as it might remove ancestry informative markers.

2. *Ultra-dimensionality* (or ultra-high-dimensionality), which refers to the scenario in which the sample-to-marker ratio n/p is nearly zero. In the random matrix theory literature, this is essentially a different regime from the one used in the PCA-TW test which assumes that n and p are comparably large ([Johnstone, 2001](#)). A genotype sequencing data set typically includes millions of markers, which makes the ratio n/p goes to an order of 10^{-4} or even smaller. In the scenario of ultra-dimensionality, using the effective number of markers to obtain a reduced number of markers only works in certain special settings, but can become ill-posed in other settings ([Zhou et al., 2018](#)).

So far, several extensions of the PCA-TW test have been proposed. [Shriner \(2012\)](#) proposed an alternative plug-in estimate of the effective number of markers for the PCA-TW test. However, the reason why choosing such plug-in estimate has not been theoretically justified. [Zhou et al. \(2018\)](#) proposed two modified methods to improve the PCA-TW test. The first one is the model-based method that tries to reduce the influence of the LD by correcting for the local correlation structure with an alternative eigenvalue limiting distribution. However, the simple discrete distribution of the population truth in the alternative model is chosen without theoretical justification. Their second method is to use block

permutation to find out an appropriate null eigenvalue distribution. But this approach is computationally intensive and might not be computationally feasible for large-scale sequencing data.

The PCA-TW test and its extensions by [Shriner \(2012\)](#) and [Zhou et al. \(2018\)](#) all share one common key idea, that is, the sample covariance matrix can be viewed as a *finite rank perturbation* of the sample noise covariance matrix. The theory of finite-rank perturbation of a large random matrix originates from the seminal spiked population model introduced by [Johnstone \(2001\)](#). After that, there are subsequent important developments ([Paul, 2007](#); [Baik and Silverstein, 2006](#); [Baik et al., 2005](#); [Bai and Yao, 2008](#); [Benaych-Georges and Nadakuditi, 2011](#); [Benaych-Georges et al., 2011](#)). The theory essentially states that the non-zero ordered eigenvalues of the sample covariance matrix \mathbf{S}_n can be separated into two parts: (1) the largest few ones are called *spikes*, whose number is exactly equal to the number of sub-populations minus one; (2) the remaining ones are called *bulk*, which asymptotically form a dense distribution well-separated from the spikes. Therefore, the null distribution of the top bulk eigenvalue can be used to detect spikes and to estimate the number of sub-populations.

Unlike the PCA-TW test and its aforementioned extensions, several researchers proposed to use the ratio (or more generally, ratio-wise functions) of the consecutive eigenvalues ($\ell_1 \geq \ell_2 \geq \dots \geq \ell_n > 0$) as a more robust test statistic to detect spikes. An estimator using the ratio of eigenvalue differences $(\ell_i - \ell_{i+1})/(\ell_{i+1} - \ell_{i+2})$ as the test statistic was first proposed by [Onatski \(2009\)](#) to estimate the number of factors. Later, [Lam and Yao \(2012\)](#) and [Ahn and Horenstein \(2013\)](#) proposed an eigenvalue ratio (ER) based estimator $\text{argmax}_{i \leq K_{\max}} \ell_i / \ell_{i+1}$ given a pre-determined K_{\max} . Another type of ER-based estimator $\min\{i \geq 1 \text{ s.t. } \ell_i / \ell_{i+1} > 1 - d_T\}$ was proposed by [Li et al. \(2017\)](#), where d_T is chosen within $(0, 1)$. These previous results all show substantial improvements for spike detection. However, previous works on ER-based estimators focus mainly on moderate-to-high dimensional data sets with mild correlations between features. Particularly, these works still require that the sample size n and the number of features p be of comparable magnitude. For example, the return of stocks data being used in ([Li et al., 2017](#)) has a sample-to-factor

ratio of 16.89. Thus, they are not applicable to modern ultra-dimensional sequencing data sets where $p \gg n$, together with complicated correlation structures among features.

In this paper, we proposed a novel ER-based estimator to infer latent population structure (*ERStruct*) from ultra-dimensional sequencing data in the framework of analysis of variance (ANOVA) model by leveraging the fact that different (latent) sub-populations have different minor allele frequencies (MAF). Although, our ER-based estimator is inspired by [Li et al. \(2017\)](#), however our approach makes two new methodological contributions. First, by leveraging the recent theoretical results from random matrix theory ([Benaych-Georges and Nadakuditi, 2011](#); [Benaych-Georges et al., 2011](#); [Wang and Paul, 2014](#)), we find a new way to approximate the distribution of the eigenvalues of the sample covariance matrix under ultra-dimensionality regime by the distribution of the eigenvalues of a high-dimensional Gaussian orthogonal ensemble (GOE) matrix. Then, we use the known random matrix theory under high-dimensional regime to dig out an adaptive approximation to the true null distribution, which also greatly reduces the computational burden. Second, we further resolve the LD problem in the sequencing data sets by proposing new estimates of the parameters in the approximation theory developed by [Wang and Paul \(2014\)](#) and obtain an LD-adjusted null distribution under the ultra-dimensional regime. We conduct simulation studies to compare our ERStruct method with the traditional PCA-TW test. Further, we apply our ERStruct method to the HapMap 3 data set ([The International HapMap 3 Consortium, 2010](#)) and the 1000 Genomes Project sequencing data set ([The 1000 Genomes Project Consortium, 2015](#)). Our proposed ERStruct method has been found to be highly accurate and robust, and is also computationally efficient. We implemented the ERStruct method as a MATLAB toolbox publicly available at <https://github.com/bglvly/ERStruct>.

In the rest of the paper, we introduce the proposed ERStruct method and computational algorithm in Section 2. In Section 3, we perform simulation studies to compare our ERStruct method with the traditional PCA-TW test. In Section 4, we apply our ERStruct method to two real data sets and compare its performance with the PCA-TW test. This paper ends with discussions in Section 5.

2 Method

Suppose that one is interested in estimating the number of sub-populations based on a raw n -by- p genotype matrix \mathbf{C} which contains p genetic markers from n individuals. Each entry $\mathbf{C}(i, j) \in \{0, 1, 2\}$ represents the raw count of the minor alleles for the genetic marker j on the individual i . Assume that there are K unknown (or latent) sub-populations and the k th sub-population is of size n_k , where $\sum_k n_k = n$ and $1 \leq k \leq K$. To refer to sub-population specific individuals, the index of individual i is written as follows:

$$i = (k, l), \quad k = 1, \dots, K \quad \text{and} \quad l = 1, \dots, n_k,$$

where k indexed the latent sub-populations and l indexed the individuals in the k th sub-population. Using this notation, the raw count matrix \mathbf{C} can be rewritten as

$$\mathbf{C} = (\underbrace{\mathbf{c}_{1,1}^\top, \dots, \mathbf{c}_{1,n_1}^\top}_{\text{1st sub-pop}}, \underbrace{\mathbf{c}_{2,1}^\top, \dots, \mathbf{c}_{2,n_2}^\top, \dots, \dots, \dots, \mathbf{c}_{K,1}^\top, \dots, \mathbf{c}_{K,n_K}^\top}_{\text{2nd sub-pop}})^\top, \underbrace{\dots}_{K\text{th sub-pop}}$$

where $\mathbf{c}_{k,l} \equiv \mathbf{C}(i, \cdot)$ is a p -dimensional vector containing information of the genetic variants for the i th individual. We consider the following asymptotic regime throughout this paper.

ASYMPTOTIC REGIME A:

$$\begin{cases} \text{sample size } n \rightarrow \infty, \\ \text{sample-to-marker ratio } n/p \rightarrow 0. \end{cases}$$

This asymptotic regime is reasonable in sequencing data, where the number of markers p is far greater than the sample size n .

2.1 Modeling Framework

Our model builds on the key fact that individuals from different sub-populations have different minor allele frequencies (MAF) and individuals from the same sub-population have the same MAF. This observation motivates us to model the raw minor allele count data matrix using the following analysis of variance (ANOVA) model,

$$\mathbf{c}_{k,l} = \boldsymbol{\mu}_k + \boldsymbol{\varepsilon}_{k,l}, \quad (1)$$

where the p -dimensional vectors $\boldsymbol{\mu}_1, \dots, \boldsymbol{\mu}_K$ are the sub-population-specific mean counts of minor alleles across the K latent sub-populations, and the vectors $\boldsymbol{\varepsilon}_{1,1}, \dots, \boldsymbol{\varepsilon}_{K,n_K}$ are independent and identically distributed noise vectors with mean zeros and covariance $\boldsymbol{\Sigma}$. We emphasize here that even though we use this ANOVA model for the raw minor allele count matrix, however our model differs from the classical ANOVA model in three ways. First, we do not know the total number of sub-populations K a priori and which individual belongs to which sub-population. Second, the sample to marker ratio n/p is nearly zero. Third, our model allows for the presence of different LD patterns. Those three salient features of our ANOVA model thus require modern random matrix theory to understand the sources of the variation in the sequencing data.

Following [Patterson et al. \(2006\)](#), we normalize the raw count matrix \mathbf{C} such that each column (genetic marker) has mean zero and unit variance. The estimates of the k th sub-population-specific mean vector $\hat{\boldsymbol{\mu}}_k$ and the estimate of the overall mean vector $\hat{\boldsymbol{\mu}}$ are given by

$$\begin{aligned}\hat{\boldsymbol{\mu}}_k &= \frac{1}{n_k} \sum_{l=1}^{n_k} \mathbf{c}_{k,l}, \\ \hat{\boldsymbol{\mu}} &= \frac{1}{n} \sum_{k=1}^K \sum_{l=1}^{n_k} \mathbf{c}_{k,l} = (\hat{\mu}_1, \dots, \hat{\mu}_p)^T.\end{aligned}\tag{2}$$

We also need the following diagonal matrix with diagonal elements equal to the standard deviations of the p genetic markers

$$\hat{\mathbf{D}} = \text{diag}\left(1/\sqrt{\hat{\mu}_j(1-\hat{\mu}_j/2)}\right), \quad 1 \leq j \leq p.$$

Then the normalized genotype data matrix is given by

$$\mathbf{M} = \begin{pmatrix} \mathbf{m}_{1,1} \\ \vdots \\ \mathbf{m}_{K,n_K} \end{pmatrix} = \begin{pmatrix} \hat{\mathbf{D}} \cdot (\mathbf{c}_{1,1} - \hat{\boldsymbol{\mu}}) \\ \vdots \\ \hat{\mathbf{D}} \cdot (\mathbf{c}_{K,n_K} - \hat{\boldsymbol{\mu}}) \end{pmatrix}.\tag{3}$$

Define the sample covariance matrix of the normalized data as $\mathbf{S}_n = \frac{1}{n} \mathbf{M} \mathbf{M}^T$. Then, we have the following standard ANOVA decomposition

$$\mathbf{S}_n \equiv \mathbf{S}_B + \mathbf{S}_W,$$

where the between-group variation is given by

$$\mathbf{S}_B = \sum_{k=1}^K \frac{n_k}{n} \left(\hat{\mathbf{D}}(\hat{\boldsymbol{\mu}} - \hat{\boldsymbol{\mu}}_k) \right)^\top \left(\hat{\mathbf{D}}(\hat{\boldsymbol{\mu}} - \hat{\boldsymbol{\mu}}_k) \right),$$

and the within-group variation is given by

$$\mathbf{S}_W = \frac{1}{n} \sum_{k=1}^K \sum_{l=1}^{n_k} \left(\hat{\mathbf{D}}(\boldsymbol{\mu}_k - \hat{\boldsymbol{\mu}}_k + \boldsymbol{\varepsilon}_{k,l}) \right)^\top \left(\hat{\mathbf{D}}(\boldsymbol{\mu}_k - \hat{\boldsymbol{\mu}}_k + \boldsymbol{\varepsilon}_{k,l}) \right). \quad (4)$$

In the next section, we will perform spectral analysis for \mathbf{S}_n using modern random matrix theory.

2.2 The Spikes and the Bulk

It can be seen from Equation (4) that the within-group covariance matrix \mathbf{S}_W is essentially the noise covariance matrix. The between-group covariance matrix \mathbf{S}_B is of rank $K-1$ because it is the sum of K rank one matrices and those K between-group vectors $\{\hat{\mathbf{D}}(\hat{\boldsymbol{\mu}}_k - \hat{\boldsymbol{\mu}})\}_K$ satisfy the following linear constraint:

$$\sum_{k=1}^K \frac{n_k}{n} \hat{\mathbf{D}}(\hat{\boldsymbol{\mu}}_k - \hat{\boldsymbol{\mu}}) = \hat{\mathbf{D}} \cdot \mathbf{0} = \mathbf{0}.$$

Hence the matrix \mathbf{S}_n can be viewed as a $K-1$ rank perturbation of the sample noise covariance matrix \mathbf{S}_W . According to the finite-rank perturbation theory (Benaych-Georges and Nadakuditi, 2011; Benaych-Georges et al., 2011), under the assumption that $\min_{k \neq k^*} \|\boldsymbol{\mu}_k - \boldsymbol{\mu}_{k^*}\| \rightarrow \infty$, the non-zero ordered sample eigenvalues $\ell_1 \geq \dots \geq \ell_{n-1} > 0$ of matrix \mathbf{S}_n can be separated into two sets by relating them to the eigenvalues of either \mathbf{S}_B or \mathbf{S}_W (graphically illustrated in Figure 1):

1. The major part of the non-zero eigenvalues $\ell_K \geq \dots \geq \ell_{n-1} > 0$ of \mathbf{S}_n , which are infinitely many as $n \rightarrow \infty$, will converge on a closed interval $[a, b] \subseteq (0, \infty)$ to the same limiting distribution of eigenvalues of the within-group covariance matrix \mathbf{S}_W . This compact set of eigenvalues is therefore called the bulk.

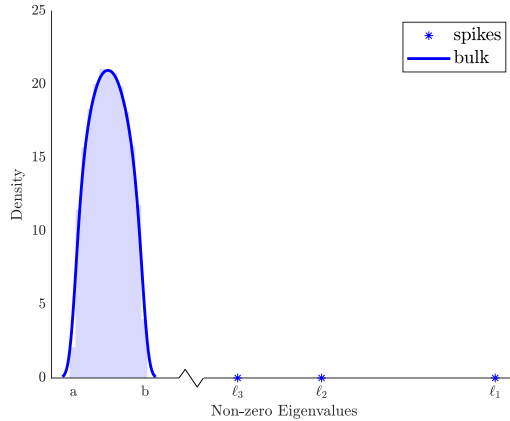


Figure 1: A typical distribution of non-zero sample eigenvalues of sample covariance matrix \mathbf{S}_n (or equivalently \mathbf{S}_p) computed from an ultra-dimensional data generated based on the uncorrelated simulation setting discussed in Section 3 (except that for a clearer view, the true number of sub-populations is chosen as $K = 4$ and the size of all the sub-populations are $n_k = \{550, 600, 650, 700\}$). The broken line in the middle of the x-axis indicates a big gap between the spikes and the bulk.

2. The top $K-1$ eigenvalues $\ell_1 \geq \dots \geq \ell_{K-1}$ of \mathbf{S}_n will converge to certain limits $\lambda_1 \geq \dots \geq \lambda_{K-1} > b$, where b is the upper bound of the bulk. The top $K-1$ eigenvalues are called the spikes which are induced by the $K-1$ eigenvalues of the between-group covariance matrix \mathbf{S}_B .

Note that the matrix $\mathbf{S}_p = \frac{1}{p} \mathbf{M} \mathbf{M}^\top$ has the same non-zero eigenvalues as the matrix \mathbf{S}_n , but it is much easier to compute in practice as its dimension ($n \times n$) is much smaller than the dimension ($p \times p$) of \mathbf{S}_n . In what follows, we will use the matrix \mathbf{S}_p for computing the sample eigenvalues, and we can infer the number of sub-populations K by performing spectral analysis on the matrix \mathbf{S}_p .

As a consequence, for any finite number m that satisfies $K \leq m \ll n$, we have the following results hold (almost surely) (Benaych-Georges and Nadakuditi, 2011)

$$\begin{cases} \ell_i \rightarrow \lambda_i, & 1 \leq i \leq K-1, \\ \ell_i \rightarrow b, & K \leq i \leq m. \end{cases}$$

In particular, if we let $\lambda_K = b$ and define the ratio of the sample eigenvalue limit as $\theta_i = \lambda_{i+1}/\lambda_i$, then for the sample ERs $r_i = \ell_{i+1}/\ell_i$, we have the following convergence results

$$\begin{cases} r_i \rightarrow \theta_i < 1, & 1 \leq i \leq K-1, \\ r_i \rightarrow b/b = 1, & K \leq i \leq m. \end{cases} \quad (5)$$

To avoid confusions with bulk and spike, which are typically used for eigenvalues, we will refer to the ratio r_i as the spiked ER when $1 \leq i \leq K-1$, and as the bulk ER when $K \leq i \leq n-1$ (the last ER r_n is 0 by definition).

2.3 The ER-based Estimator

Based on the above asymptotic results, theoretically we can leverage the asymptotically consistent ER-based estimator studied in (Li et al., 2017) to estimate the number of latent sub-populations K as follows

$$\hat{K}'_{ER} := \min\{1 \leq i \leq n-1 \text{ s.t. } r_i > \xi_\alpha\}, \quad (6)$$

where α is the pre-specified significance level, and the critical value ξ_α is chosen as the lower α quantile of the distribution of the top bulk ER r_K (as illustrated in Figure 2).

Note that by the definition in the Equation (6), the probability of overestimation (i.e., spurious detection on the bulk side) of our proposed estimator \hat{K}'_{ER} is controlled by the significance level α . However, there is no such control on the probability of underestimation (i.e., spurious detection on the spiked side). Underestimation might occur when the largest spiked ER $\max_{1 \leq i < K} \{r_i\}$ jumps above the critical value ξ_α , leading to an early stop of our sequential testing procedure as given in Equation (6). Thus, in order to control the probability of underestimation, we need to know the theoretical joint distribution of the spiked ERs. But unlike the bulk, the asymptotic distribution of the spiked eigenvalues (and thus the spiked ERs) is sensitive and varies with different distributions of the entries in the data matrix (Benaych-Georges and Nadakuditi, 2011; Benaych-Georges et al., 2011). As a result, each entry in the data matrix can substantially affect the distributions of the

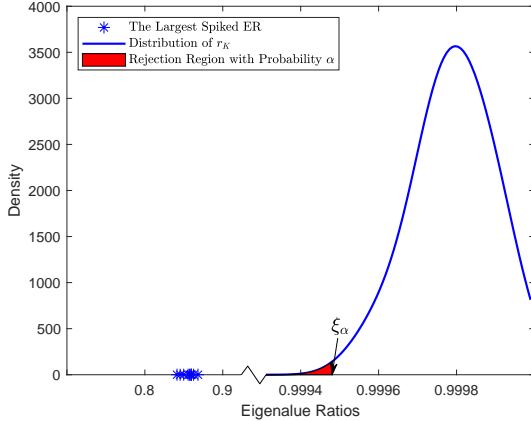


Figure 2: The largest spiked ER and the well-separated distribution of the top bulk ER r_K , generated from 100 simulations following the same setting as in Figure 1. Those ERs that are less than the critical value ξ_α will be considered as the spikes (here α is set as 0.005 for illustration).

spikes. We observe that the last spiked ER should be asymptotically less than ξ_α , while all the bulk ERs are greater than ξ_α with a probability controlled by $1-\alpha$ as in (5). With this observation, we can control the probability of underestimation by stopping the sequential testing procedure only if all the $(\hat{K}'_{ER} + 1)$ th to \hat{K}_c th eigenvalue ratios are confirmed to be above the critical value. Here, \hat{K}_c is some pre-specified coarse estimate \hat{K}_c for the number of sub-populations, which should be generally larger than the true K . By default, we set $\hat{K}_c = n/10$ in our algorithm to ensure $\hat{K}_c > K$ because for usual statistical estimations (and especially in the ultra-dimensional scenarios), it is crucial to have at least 10 samples in one sub-population to achieve decent estimation accuracy.

Another challenge when applying our ER-based estimator defined in Equation (6) to real data sets is to find out a proper value of ξ_α as the distribution of r_K is generally unknown. As we have mentioned in Section 1, the approach in (Li et al., 2017) does not work on sequencing genotype data sets because of the severe LD and ultra-dimensionality issues. We now introduce a novel method to address these two issues and then obtain a more accurate approximation for ξ_α .

According to Benaych-Georges et al. (2011), the distributions of the top two bulk eigen-

values ℓ_K and ℓ_{K+1} can be approximated by the distributions of the top two eigenvalues $\tilde{\ell}_1$ and $\tilde{\ell}_2$ of the following n -by- n noise covariance matrix respectively:

$$\tilde{\mathbf{S}}_p = \frac{1}{p} \mathbf{X} \boldsymbol{\Sigma} \mathbf{X}^\top, \quad (7)$$

where \mathbf{X} is a n -by- p random matrix with all independent and identically distributed standard Gaussian entries. Let $\tilde{r}_1 = \tilde{\ell}_2/\tilde{\ell}_1$, the above result implies that $r_K \overset{\sim}{\sim} \tilde{r}_1$, where the notation $\overset{\sim}{\sim}$ denotes that the two random variables on its two sides asymptotically follow the same distribution. Given the population covariance matrix $\boldsymbol{\Sigma}$ and a significant level α , we can in principle approximate ξ_α using the following equation

$$P(0 < \tilde{r}_1 \leq \tilde{\xi}_\alpha) = \alpha.$$

However, even if we know the true covariance $\boldsymbol{\Sigma}$, the top two eigenvalues $\tilde{\ell}_1$ and $\tilde{\ell}_2$ are essentially roots of a polynomial equation of order n whose distribution functions have no closed forms in general. It is also computationally inefficient to use Monte Carlo method to simulate the null distribution based on the covariance matrix $\tilde{\mathbf{S}}_p$ defined in Equation (7) as we need to generate a huge n -by- p matrix \mathbf{X} multiple times where p is at the order of millions. To solve this problem, we apply the limiting theory for the eigenvalues of the sample noise matrix developed by [Wang and Paul \(2014\)](#) under the Asymptotic Regime A. The theory states that the eigenvalues of $\sqrt{p/nb_p}(\tilde{\mathbf{S}}_p - a_p \mathbf{I}_n)$ converge almost surely to the *semicircle law*, where $a_p = \text{tr}(\boldsymbol{\Sigma})/p$ and $b_p = \text{tr}(\boldsymbol{\Sigma}^2)/p$ and $\text{tr}(\cdot)$ denotes the trace of a matrix. The semicircle law gives the same limiting distribution for the eigenvalues of \mathbf{W}_n/\sqrt{n} when $n \rightarrow \infty$, where \mathbf{W}_n is a n -by- n Gaussian orthogonal ensemble (GOE) matrix (i.e., a square matrix with independent entries where each diagonal entry follows $N(0, 2)$ and each off-diagonal entry follows $N(0, 1)$) ([Wigner, 1958](#); [Arnold, 1971](#)). Hence, the relationships of the top two eigenvalues of $\sqrt{p/nb_p}(\tilde{\mathbf{S}}_p - a_p \mathbf{I}_n)$ and \mathbf{W}_n/\sqrt{n} are given by

$$\sqrt{p/nb_p} \cdot (\tilde{\ell}_i - a_p) \overset{\sim}{\sim} w_i/\sqrt{n}, \quad i = 1, 2, \quad (8)$$

where w_1 and w_2 are the top two eigenvalues of matrix \mathbf{W}_n . As a result, the top bulk ER

r_K can be approximated by

$$r_K \dot{\sim} \tilde{r}_1 = \frac{\tilde{\ell}_2}{\tilde{\ell}_1} \dot{\sim} \frac{w_2 \cdot \sqrt{\hat{b}_p/p} + \hat{a}_p}{w_1 \cdot \sqrt{\hat{b}_p/p} + \hat{a}_p} = \tilde{r}_1^*, \quad (9)$$

where

$$\hat{a}_p = \frac{1}{n-K} \sum_{i=K}^{n-1} \ell_i, \quad (10)$$

$$\hat{b}_p = \frac{p}{(n-K)^2} \sum_{i=K}^{n-1} (\ell_i - \hat{a}_p)^2, \quad (11)$$

are the two moment estimators for a_p and b_p in Equation (8) respectively.

Denote $\tilde{\xi}_\alpha^*$ as the new approximation for the critical value ξ_α in Equation (6). Given a pre-specified coarse estimator $\hat{K}_c < n-1$, our final ER-based estimator for the number of sub-populations K is

$$\hat{K}_{ER} := \min \{1 \leq i \leq \hat{K}_c \text{ s.t. } r_i, \dots, r_{\hat{K}_c} \text{ all greater than } \tilde{\xi}_\alpha^*\},$$

where we choose $\tilde{\xi}_\alpha^*$ as the lower α quantile of the distribution of \tilde{r}_1^* in Equation (9), that is,

$$P(0 < \tilde{r}_1^* \leq \tilde{\xi}_\alpha^*) = \alpha.$$

2.4 ERStruct Algorithm

We summarize our method as an algorithm for estimating the number of sub-populations K from a raw genotype data matrix \mathbf{C} below.

Algorithm ERStruct

Input: \mathbf{C} $n \times p$ genotype data matrix

\hat{K}_c coarse estimate (set to $\lfloor n/10 \rfloor$ by default)

m number of replicates

α significant level

Output: \hat{K}_{ER} ER estimation of the sub-population number

```

1  $\mathbf{M} \leftarrow$  Equation (3)
2  $\mathbf{S}_p \leftarrow \frac{1}{p}\mathbf{M}\mathbf{M}^\top$ 
3  $\ell_1 \geq \ell_2 \geq \dots \geq \ell_{n-1} \leftarrow$  ordered non-zero eigenvalues of  $\mathbf{S}_p$ 
4  $(r_1, \dots, r_{n-2}) \leftarrow (\ell_2/\ell_1, \dots, \ell_{n-1}/\ell_{n-2})$ 
5  $((w_1^{(1)} \cdots w_1^{(m)})^\top, (w_2^{(1)} \cdots w_2^{(m)})^\top) \leftarrow$  generate  $m$  replicates of the top two eigenvalues
   of GOE matrices  $\mathbf{W}_n$ 
6 for  $K \leftarrow 1$  to  $\hat{K}_c$  do
7   if no valid  $\hat{K}_{ER}$  then
8      $(\hat{a}_p, \hat{b}_p) \leftarrow$  Equations (10) and (11)
9     for  $i \leftarrow 1$  to  $m$  do
10     $(w_1, w_2) \leftarrow (w_1^{(i)}, w_2^{(i)})$ 
11     $\tilde{r}_1^{*(i)} \leftarrow$  Equation (9)
12  end for
13   $\tilde{\xi}_\alpha^* \leftarrow \tilde{r}_1^{*([m\alpha])}$ 
14  if  $r_K > \tilde{\xi}_\alpha^*$  then
15     $\hat{K}_{ER} \leftarrow K$  and set  $\hat{K}_{ER}$  as valid
16  end if
17  else if  $r_K \leq \tilde{\xi}_\alpha^*$  then set  $\hat{K}_{ER}$  as not valid
18  end if
19 end for

```

3 Simulation Studies

In this section, we compare the performances of our new method ERStruct versus the traditional PCA-TW test based on their final estimated number of sub-populations. We consider two different settings depending on whether or not the LD is present.

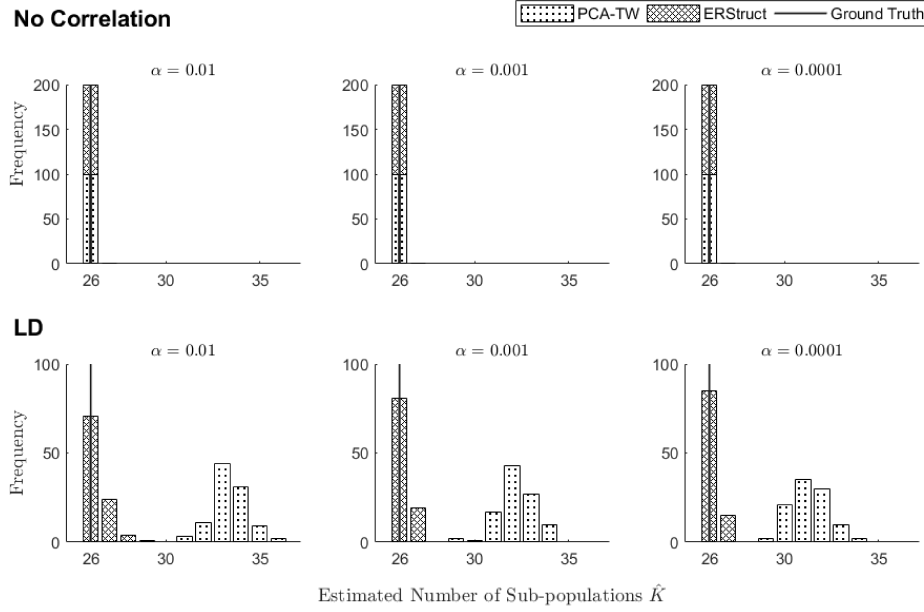


Figure 3: Histograms of the estimated number of sub-populations using the PCA-TW test (dotted) and ERStruct (crossed) in uncorrelated (upper panel) and LD settings (lower panel), each with 100 replications. The ground truth is $K = 26$.

Table 1: Simulation results for the estimated numbers of sub-populations using the PCA-TW test and ERStruct in the LD setting. The correct estimations represent the percentages of estimations that are equal to the true number (26) of sub-populations. The range denotes the minimum and maximum estimated numbers.

| α level | PCA-TW test | | | ERStruct | | |
|---------------------|-------------|----------|----------|----------|----------|----------|
| | 0.01 | 0.001 | 0.0001 | 0.01 | 0.001 | 0.0001 |
| correct estimations | 0 | 0 | 0 | 71% | 81% | 85% |
| range | [31, 36] | [29, 34] | [29, 34] | [26, 29] | [26, 27] | [26, 27] |
| bias | 7.38 | 6.22 | 5.31 | 0.35 | 0.19 | 0.15 |
| variance | 0.94 | 1.02 | 1.08 | 0.37 | 0.16 | 0.13 |

1. In the uncorrelated setting, the marker-to-marker covariance is set as $\Sigma = 0.5 \cdot \mathbf{I}_p$, and 100 independent Monte Carlo replicated samples of genotype data matrices are generated according to the ANOVA model (1). The other parameters are set so that the simulated data is similar to the 1000 Genomes Project data set with MAF less than 5% rare markers filtered out as analyzed in Section 4. Specifically, the number of markers $p = 7,921,816$; the number of individuals $n = 2504$; the number of sub-populations $K = 26$; the numbers of individuals in each sub-population $n_k = \{96, 61, 86, 93, 99, 103, 105, 94, 99, 99, 91, 103, 113, 107, 102, 104, 99, 99, 85, 64, 85, 96, 104, 102, 107, 108\}$; the noise vector $\boldsymbol{\varepsilon}_{k,l} \sim N(\mathbf{0}, 0.5 \cdot \mathbf{I}_p)$; and the mean count of minor alleles $\boldsymbol{\mu}_k \sim \text{Binomial}(2, \hat{\boldsymbol{\mu}}_k/2)$, with $\hat{\boldsymbol{\mu}}_k$ obtained by Equation (2) in which $\mathbf{c}_{k,l}$ is the raw minor allele counts of the l th individual in the k th sub-population from the 1000 Genomes Project data set. Finally, we use a rounding mapping $x \mapsto I_{x \geq 1.5}(x) - I_{x < 0.5}(x) + 1$ so that all the simulated genotype data take values in $\{0, 1, 2\}$, where $I_A(\cdot)$ denotes an indicator function on a set A .
2. In the LD setting, in order to simulate local marker-to-marker correlations (the LD matrix), the noise vectors $\boldsymbol{\varepsilon}_{k,l}$ within the k th sub-population are generated from the distribution $N(\mathbf{0}, 0.5 \cdot \Sigma_k)$. Each Σ_k is a block diagonal matrix extracted from the sample correlation matrix of the k th sub-population in the 1000 Genomes Project data set. All the other parameters (i.e., the number of markers p , the number of individuals n , the number of sub-populations K , numbers of individuals in each sub-population n_k and the mean count of minor alleles $\boldsymbol{\mu}_k$) are set to be the same values as in the uncorrelated setting.

The simulation results are shown in Figure 3 and Table 1. Our proposed ERStruct method significantly reduces the bias and variance of estimates compared to the PCA-TW test. Specifically, in the uncorrelated setting which favors the PCA-TW test, our ERStruct achieve the same accuracy as the PCA-TW test. In the LD setting, 85% ($\alpha = 0.0001$) of the replicates using ERStruct are correctly estimated, and the rest 15 replicates still give highly accurate estimates (ground truth $K = 26$ versus $\hat{K}_{ER} = 27$ when $\alpha = 0.0001$). In contrast, the PCA-TW test has no correct estimates among those 100 replicates and the

Table 2: Geographical information of HapMap 3 data set.

| Sub-population | | Sample size |
|----------------|--|-------------|
| ASW | (African ancestry in Southwest USA) | 71 |
| CEU | (Utah residents with Northern and Western European ancestry) | 162 |
| CHB | (Han Chinese in Beijing, China) | 82 |
| CHD | (Chinese in Metropolitan Denver, Colorado) | 70 |
| GIH | (Gujarati Indian in Houston, Texas) | 83 |
| JPT | (Japanese in Tokyo, Japan) | 82 |
| LWK | (Luhya in Webuye, Kenya) | 83 |
| MXL | (Mexican ancestry in Los Angeles, California) | 71 |
| MKK | (Maasai in Kinyawa, Kenya) | 171 |
| TSI | (Toscani in Italy) | 77 |
| YRI | (Yoruba in Ibadan, Nigeria) | 163 |
| consensus | | 1115 |

Table 3: Geographical information of the 1000 Genomes Project data set.

| Sub-population | | Sample size |
|----------------|--|-------------|
| ACB | (African Caribbean in Barbados) | 96 |
| ASW | (African ancestry in Southwest USA) | 61 |
| BEB | (Bengali in Bangladesh) | 86 |
| CDX | (Chinese Dai in Xishuangbanna, China) | 93 |
| CEU | (Utah residents with Northern and Western European ancestry) | 99 |
| CHB | (Han Chinese in Beijing, China) | 103 |
| CHS | (Southern Han Chinese, China) | 105 |
| CLM | (Colombian in Medellin, Colombia) | 94 |
| ESN | (Esan in Nigeria) | 99 |
| FIN | (Finnish in Finland) | 99 |
| GBR | (British in England and Scotland) | 91 |
| GIH | (Gujarati Indian in Houston, Texas) | 103 |
| GWD | (Gambian in Western Division, The Gambia) | 113 |
| IBS | (Iberian populations in Spain) | 107 |
| ITU | (Indian Telugu in the UK) | 102 |
| JPT | (Japanese in Tokyo, Japan) | 104 |
| KHV | (Kinh in Ho Chi Minh City, Vietnam) | 99 |
| LWK | (Luhya in Webuye, Kenya) | 99 |
| MSL | (Mende in Sierra Leone) | 85 |
| MXL | (Mexican ancestry in Los Angeles, California) | 64 |
| PEL | (Peruvian in Lima, Peru) | 85 |
| PJL | (Punjabi in Lahore, Pakistan) | 96 |
| PUR | (Puerto Rican in Puerto Rico) | 104 |
| STU | (Sri Lankan Tamil in the UK) | 102 |
| TSI | (Toscani in Italy) | 107 |
| YRI | (Yoruba in Ibadan, Nigeria) | 108 |
| consensus | | 2504 |

results are far away from the ground truth (ranging from 29 to 34 even when $\alpha = 0.0001$).

4 Real Data Analysis

In this section, we apply our proposed ERStruct to two genotype data sets to estimate the number of sub-populations for illustration. We also include the PCA-TW method for comparison purpose.

The first data set is the HapMap 3 ([The International HapMap 3 Consortium, 2010](#)) project, which is a large-scale array-based genotype data set that includes 11 featured sub-populations and 1115 individuals around the world (see Table 2 for a more detailed geographical information). Although the interest of this paper is in large-scale sequencing data, HapMap 3 includes such a large number of markers (1,615,203 for the raw data in total) that the sample-to-marker ratio of the raw data is sufficiently small ($n/p = 6.9 \times 10^{-4}$). Therefore, the HapMap 3 data set can be considered as falling into our ultra-dimension Asymptotic Regime A. The HapMap 3 data set used in our analysis is publicly accessible at <https://www.sanger.ac.uk/resources/downloads/human/hapmap3.html>.

The second one is the 1000 Genomes Project ([The 1000 Genomes Project Consortium, 2015](#)), which is a whole-genome sequencing data set with 26 sub-populations and 2504 individuals (detailed geographical information shown in Table 3). It is established in January 2008 with the aim to build by then the most detailed catalogue of genetic variations in the human population. The 1000 Genomes Project inherits the major part of the data in HapMap 3, with additional featured sub-populations and a lot of rarer genetic variants (81,271,745 for the raw data in total) involved. In this section, we analyze the data from the phase 3 v5a of the 1000 Genomes Project, which is publicly accessible at <https://www.internationalgenome.org/data>.

Our raw data pre-processing is as follows. We first filter rare genetic markers using the PLINK software ([Purcell et al., 2007](#)) to obtain different levels of LD pruning/clumping. For HapMap 3, markers with MAF less than (5%, 1%) are removed. For the 1000 Genomes Project sequencing data set, we also investigate several situations in which we remove rarer markers with MAF less than (5%, 1%, 0.5%, 0.1%, 0.05%, 0.01%). Then under different

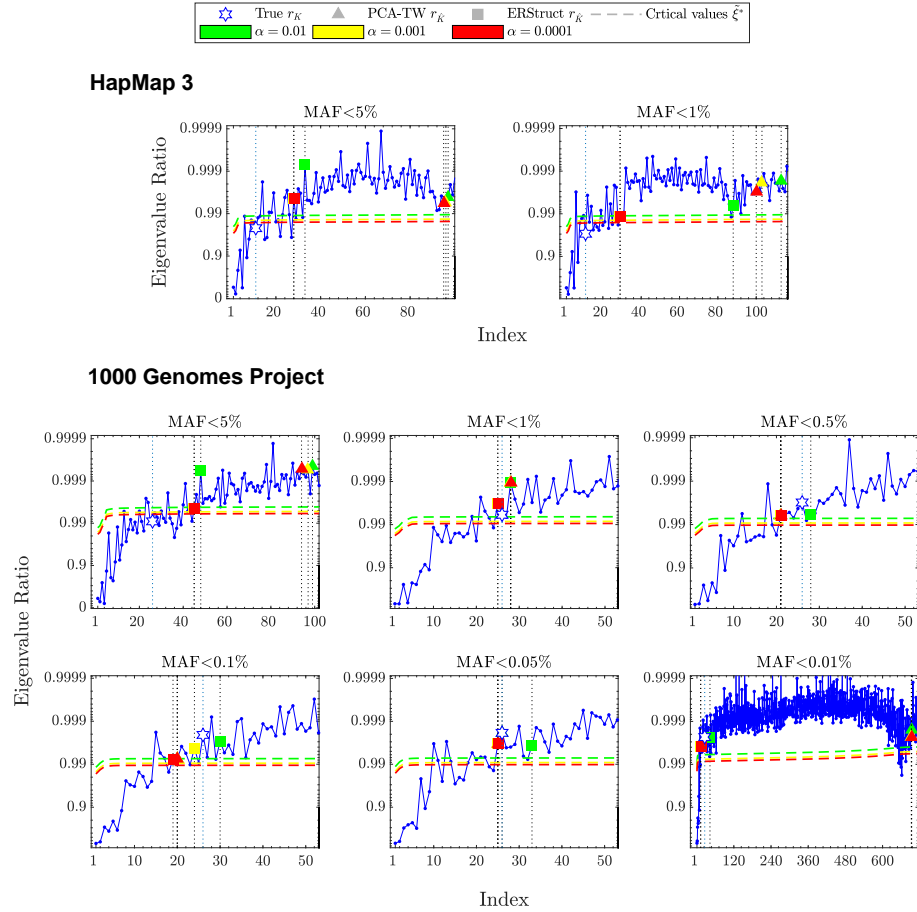


Figure 4: Scree plots of ERs computed from the HapMap 3 (11 sub-populations) and 1000 Genomes Project (26 sub-populations) data sets on y-axis transformed by $y \mapsto -\log_{10}(1-y)$. Each sub-plots are created based on different filtering thresholds on the raw data. Top bulk ERs that correspond to estimations with $\alpha=0.01$ (red), $\alpha=0.001$ (yellow) and $\alpha=0.0001$ (green) using the PCA-TW test (triangle) and ERStruct (square) are emphasized on the plots. This figure appears in color in the electronic version of this article, and color refers to that version.

Table 4: Comparison of estimations based on different filtering thresholds of the raw HapMap 3 (1,615,203 markers) and 1000 Genomes Project (81,271,745 markers) data sets using the PCA-TW test and ERStruct method.

| | filtered markers | n -to- p ratio | α level | PCA-TW test | | | ERStruct | | |
|-------------------------|------------------|-----------------------|----------------|-------------|-------|--------|----------|-------|--------|
| | | | | 0.01 | 0.001 | 0.0001 | 0.01 | 0.001 | 0.0001 |
| HapMap 3 | MAF < 5% | 7.47×10^{-4} | 97 | 96 | 95 | 33 | 28 | 28 | |
| | MAF < 1% | 6.96×10^{-4} | 113 | 103 | 100 | 88 | 29 | 29 | |
| 1000 Genomes Project | MAF < 5% | 3.16×10^{-4} | 99 | 97 | 94 | 48 | 45 | 45 | |
| | MAF < 1% | 1.83×10^{-4} | 28 | 28 | 28 | 28 | 25 | 25 | |
| | MAF < 0.5% | 1.44×10^{-4} | 21 | 21 | 21 | 28 | 21 | 21 | |
| | MAF < 0.1% | 8.70×10^{-5} | 20 | 20 | 20 | 24 | 24 | 19 | |
| | MAF < 0.05% | 6.60×10^{-5} | 26 | 25 | 25 | 33 | 25 | 25 | |
| | MAF < 0.01% | 3.09×10^{-5} | 694 | 693 | 693 | 43 | 13 | 13 | |

significant levels (0.01, 0.001, 0.0001), we applied the traditional PCA-TW method and our ERStruct method to the filtered HapMap 3 and the 1000 Genomes Project data sets.

As shown in Figure 4, all the ER scree plots are oscillating curves with no specific patterns around the ground truth top bulk ER. This shows the need to estimate the number of sub-populations through using more rigorous statistical inference method and the simple eyeballing method is not sufficient here. More detailed estimation results are summarized in Table 4. Under almost all settings, our ERStruct gives closer estimations to the ground truth. In comparison, the PCA-TW test results in severe over-estimation on the 1000 Genome Project data set with more (MAF less than 5%) or less (MAF less than 0.01%) markers filtered. The problem of over-estimation remains on all filtering thresholds of the smaller HapMap 3 data set, which has sample-to-marker ratios closer to the asymptotic regime assumed in the PCA-TW test ($n/p \rightarrow \text{constant}$). These results coincide with our conclusions in Section 3, and further suggest strong robustness of our ERStruct method to both information losses (i.e., with more markers filtered than needed) and noise perturbations (fewer markers filtered).

5 Discussion

The traditional PCA-TW test was originally developed for array-based genotype data set where the number of genetic markers is much smaller than that from modern sequencing data (Patterson et al., 2006). Hence, the PCA-TW method has been found to perform not well when the sample to marker ratio is nearly zero as in the sequencing data. Our proposed method ERStruct has been shown to outperform the traditional PCA-TW test in both simulated and real sequencing data.

Our ERStruct method enjoys several advantages. First, our ERStruct estimator is based on the more robust eigenvalue ratios. Second, we obtain a closer adaptive null distribution for the ER test statistic under the ultra-dimensional regime which is specifically developed for modern sequencing data. Third, our method is not confined to a specific LD structure among genetic markers. Even though in the real genetic data with complicated LD structures, our ERStruct can still separate the spikes from the bulk. Fourth, our ERStruct method is also computationally efficient. In fact, our ERStruct achieves almost the same computational speed as the PCA-TW test, given that $p \gg n$. For example, it took only around 30 minutes to obtain the estimate of the 1000 Genomes Project data set with MAF less than 0.05% filtered (37,961,945 markers) using our ERStruct MATLAB toolbox on a sever with 126G RAM and 5 cores of CPU.

Our proposed ERStruct method can also be used for inferring latent structures (like the number of latent batches) in other types of ultra-dimensional genetic/genomic data. However, both our proposed ERStruct method and the PCA-TW test are developed for population-based genotype data. In single-cell sequencing data, most of the entries in the data matrix are zeros. Inference of latent structures in such sparse data matrix is still very challenging because such zero-inflated data matrix will seriously distort the null distribution of the ER test statistic (Hwang et al., 2019; Aparicio et al., 2020). Even though in Section 4, our ERStruct method shows decent robustness to sparse data sets, more future work is needed to further boost the performance of ERStruct by accounting for the sparsity issue under the ultra-dimensional regime.

References

Ahn, S. C. and A. R. Horenstein (2013). Eigenvalue ratio test for the number of factors. *Econometrica* 81(3), 1203–1227.

Aparicio, L., M. Bordyuh, A. J. Blumberg, and R. Rabadian (2020). A random matrix theory approach to denoise single-cell data. *Patterns* 1(3), 100035.

Arnold, L. (1971). On Wigner’s semicircle law for the eigenvalues of random matrices. *Probability Theory and Related Fields* 19(3), 191–198.

Bai, Z. and J. Yao (2008). Central limit theorems for eigenvalues in a spiked population model. *Annales de l’IHP Probabilités et Statistiques* 44(3), 447–474.

Baik, J., G. B. Arous, and S. Péché (2005). Phase transition of the largest eigenvalue for nonnull complex sample covariance matrices. *The Annals of Probability* 33(5), 1643–1697.

Baik, J. and J. W. Silverstein (2006). Eigenvalues of large sample covariance matrices of spiked population models. *Journal of Multivariate Analysis* 97(6), 1382–1408.

Benaych-Georges, F., A. Guionnet, and M. Maida (2011). Fluctuations of the extreme eigenvalues of finite rank deformations of random matrices. *Electronic Journal of Probability* 16(60), 1621–1662.

Benaych-Georges, F. and R. R. Nadakuditi (2011). The eigenvalues and eigenvectors of finite, low rank perturbations of large random matrices. *Advances in Mathematics* 227(1), 494–521.

Cao, Y., L. Li, Z. Feng, X. Sun, J. Lu, Y. Xu, et al. (2020, Sep). The chinamap analytics of deep whole genome sequences in 10,588 individuals. *Cell Research* 30(9), 717–731.

Hwang, J. Y., J. O. Lee, and K. Schnelli (2019). Local law and Tracy–Widom limit for sparse sample covariance matrices. *The Annals of Applied Probability* 29(5), 3006–3036.

Johnstone, I. M. (2001). On the distribution of the largest eigenvalue in principal components analysis. *The Annals of Statistics* 29(2), 295–327.

Lam, C. and Q. Yao (2012). Factor modeling for high-dimensional time series: Inference for the number of factors. *The Annals of Statistics* 40(2), 694–726.

Li, Z., Q. Wang, and J. Yao (2017). Identifying the number of factors from singular values of a large sample auto-covariance matrix. *The Annals of Statistics* 45(1), 257–288.

Menozzi, P., A. Piazza, and L. Cavalli-Sforza (1978). Synthetic maps of human gene frequencies in Europeans. *Science* 201(4358), 786–792.

Novembre, J., T. Johnson, K. Bryc, Z. Kutalik, A. R. Boyko, A. Auton, et al. (2008). Genes mirror geography within Europe. *Nature* 456(7218), 98.

Onatski, A. (2009). Testing hypotheses about the number of factors in large factor models. *Econometrica* 77(5), 1447–1479.

Palla, L. and F. Dudbridge (2015). A fast method that uses polygenic scores to estimate the variance explained by genome-wide marker panels and the proportion of variants affecting a trait. *The American Journal of Human Genetics* 97(2), 250–259.

Patterson, N., A. L. Price, and D. Reich (2006). Population structure and eigenanalysis. *PLoS Genetics* 2(12), e190.

Paul, D. (2007). Asymptotics of sample eigenstructure for a large dimensional spiked covariance model. *Statistica Sinica* 17(4), 1617–1642.

Price, A. L., N. J. Patterson, R. M. Plenge, M. E. Weinblatt, N. A. Shadick, and D. Reich (2006). Principal components analysis corrects for stratification in genome-wide association studies. *Nature Genetics* 38(8), 904.

Prokopenko, D., J. Hecker, E. K. Silverman, M. Pagano, M. M. Nöthen, C. Dina, et al. (2015, 12). Utilizing the Jaccard index to reveal population stratification in sequencing data: A simulation study and an application to the 1000 Genomes Project. *Bioinformatics* 32(9), 1366–1372.

Purcell, S., B. Neale, K. Todd-Brown, L. Thomas, M. A. Ferreira, D. Bender, et al. (2007). PLINK: A tool set for whole-genome association and population-based linkage analyses. *The American Journal of Human Genetics* 81(3), 559–575.

Reich, D., A. L. Price, and N. Patterson (2008). Principal component analysis of genetic data. *Nature Genetics* 40(5), 491–492.

Shriner, D. (2012). Improved eigenanalysis of discrete subpopulations and admixture using the minimum average partial test. *Human Heredity* 73(2), 73–83.

Skoglund, P., J. C. Thompson, M. E. Prendergast, A. Mitnik, K. Sirak, M. Hajdinjak, et al. (2017, Sep). Reconstructing prehistoric african population structure. *Cell* 171(1), 59–71.e21.

Song, M., W. Hao, and J. D. Storey (2015). Testing for genetic associations in arbitrarily structured populations. *Nature Genetics* 47(5), 550.

The 1000 Genomes Project Consortium (2015). A global reference for human genetic variation. *Nature* 526(7571), 68–74.

The International HapMap 3 Consortium (2010). Integrating common and rare genetic variation in diverse human populations. *Nature* 467, 52–58.

Wang, L. and D. Paul (2014). Limiting spectral distribution of renormalized separable sample covariance matrices when $p/n \rightarrow 0$. *Journal of Multivariate Analysis* 126, 25–52.

Wigner, E. P. (1958). On the distribution of the roots of certain symmetric matrices. *Annals of Mathematics* 67(2), 325–327.

Zhang, D., R. Dey, and S. Lee (2020, 03). Fast and robust ancestry prediction using principal component analysis. *Bioinformatics* 36(11), 3439–3446.

Zhou, Y.-H., J. Marron, and F. A. Wright (2018). Eigenvalue significance testing for genetic association. *Biometrics* 74(2), 439–447.